Full Tensor Gradient (FTG) gravity data application in karst features detection in the northeastern Delaware Basin, west Texas

Hualing Zhang[1,2], Dale E. Bird[2,3]*

1. Research Institute of Petroleum Exploration & Development, PetroChina. 2. Department of Earth and Atmospheric Sciences, University of Houston. 3. Bird Geophysical.

Summary

Extensive karst development in carbonate and evaporate strata are mainly associated with the late Permian Guadalupian and Ochoan strata of the Delaware Basin, west Texas. Subsurface karst feature detection is essential because they may cause severe drilling geohazards. The objective of this study is to interpret high-resolution FTG gravity data to infer dissolution karsting related caverns, systems of caverns, and zones with high porosity in the less studied northeastern Delaware Basin. Our interpretation methods, which integrate Txz, Tyz, Tzz FTG components and subsurface geological measurements, can be utilized across assets with similar near surface geology around the world.

Introduction

The Permian Basin of West Texas and southeast New Mexico is located in the foreland area of the Ouachita-Marathon fold-thrust belt, and it is divided into three major structural components: the Delaware and Midland Basins are separated by the Central Basin Platform on the west and east, respectively (Fig 1a). Extensive karst development in carbonate and evaporate strata occur in shallow sediments of the Delaware Basin and are mainly associated with late Permian Guadalupian and Ochoan strata (Stafford, 2017; Fig 1b). Recent studies of hypogenic karst features have focused on outcrops (Ochoan Castile and Rustler formations) within the western and central Delaware Basin (e.g., Scholle et al., 2004; Stafford, 2017; Majzoub et al., 2017; Stafford et al., 2018). However, in the eastern portion of the Delaware Basin, much of the soluble rock is buried beneath northeast dipping strata of Guadalupian and Ochoan age (Fig 1b, c), so the potentially karsted Castile and Rustler Formations remain less understood.

Hypogenic karst features are often linked to geohazards during drilling operations in the highly productive Permian Basin (Dutton et al., 2004, 2005). For example, Morgan et al. (2018) reported that a drilling operator in Culbertson County, western Delaware Basin, experienced significant drilling fluid loss in several wells after penetrating open voids in the initial 500 feet of drilling. As a result, the drillers were forced to abandon the boreholes.

High-resolution, high-precision FTG data is an exploration tool used to detect and map source bodies defined by subtle density contrasts - especially those within close proximity to the measurement platform. The short wavelength resolution of FTG enables delineation of small density sources required for detailed hydrocarbon and mineral exploration. Our study applies high-resolution FTG gravity data to infer dissolution karsting related caverns, systems of caverns, and zones with high porosity in the Ruslter, Salado and Castile Formation of the late Permian Ochoan age in the northeastern Delaware Basin (Fig 1c). Results presented here demonstrate how FTG data can be applied to de-risk karst-related geohazards.

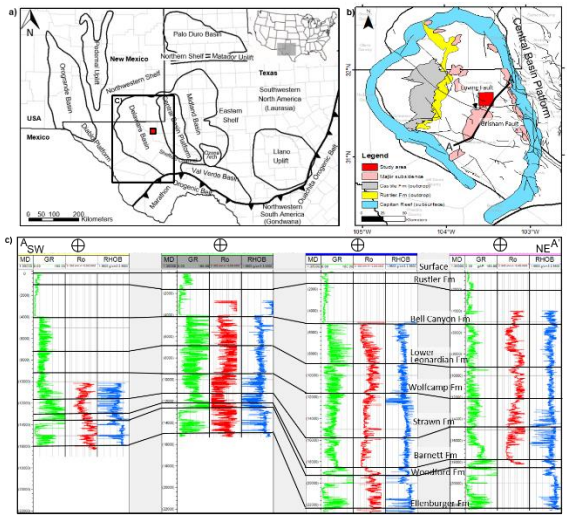

Fig 1: Geological settings of the Permian Basin and the FTG study area. a) Physiographic setting of the Permian Basin region with major basin names and the study area outlined by the red box (modified from Zhang et al., 2021). b) Geological map of select major units, related to hypogenic karst features, in the Delaware Basin. Paleozoic fault distribution (thin black lines) was mapped by Ruppel et al. (2008) and Ewing (2019), including the Grisham and Loving Faults. c) d) Well log correlated cross-section through the study area showing the stratigraphic units in the northeastern Delaware Basin deepening to the northeast.

Theory and Method

We use an airborne terrain-corrected FTG gravity survey flown by Bell Geospace over about 144 km2 over intersecting parts of Loving, Ward, and Reeves Counties. Nine well logs, provided by Enverus, are projected into the survey area for stratigraphic, lithological, and density control. Gravity gradient data are processed to follow the North-East-Down (NED) standard (Bell et al., 1997) as shown by the test model in Fig 2. That is, Txz is calculated

from west to east, and Tyz is calculated from south to north. The test model shows FTG anomalies over a low-density prism to simulate a karst feature. Note that Txz anomalies are produced by density contrasts that trend roughly N-S, and Tyz anomalies are produced by density contrasts that trend roughly E-W. The profile below the test model in Fig 2 shows Txz and Tyz anomaly profiles from west to east and south to north. Anomaly closures peaks are produced over the edges of the low-density prism in the test model.

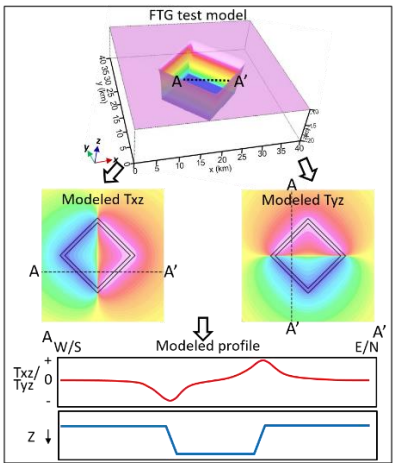

Fig 2: Test model shows the response of Txz and Tyz component anomalies over a low-density prism. Plan-view dashed lines are identical, relative component anomalies, and are therefore represented by a single cross-section below. Anomalies along these lines overlie the same structural trends, following the NED calculation standard.

All 3D FTG models are constructed with Seequent's Oasis Montaj software, which employs forward and inverse frequency-domain algorithms. The models include ten layers: seven sedimentary from the surface to the Top Ellenburger Formation, two crystalline crusts, and an upper mantle. Structural and density grids for the FTG model are extracted from a regional, basin-scale 3D model in the Permian Basin (Zhang et al., 2021; Fig 3). In this basin-scale model, formation tops of each sedimentary layer are correlated from 296 well logs throughout the Permian Basin and then gridded to 4km cells (Zhang et al., 2021; Fig 3). Average density values within each layer are calculated at each well location (1614 measurements) and also gridded to 4km cells (Zhang et al., 2021). The densities of upper crust, lower crust, and upper mantle used in the regional model are 2.75, 2.9, 3.3 gm/cc, respectively (Zhang et al., 2021).

A structural inversion of the Moho horizon was first conducted to improve the long-wavelength crustal geometry in the study area. Then, density inversions of gravity (Tz) anomalies were calculated for the top two sedimentary layers individually (topography to top Rustler, and top Rustler to top Leonardian), as well as these layers combined (topography to top Leonardian). After achieving a satisfactory Tz inversion result (RMS difference between calculated and measured data < 0.8 mGal), density inversions of the Tzz gradient component are conducted to capture more subtle density variations within each sedimentary layer.

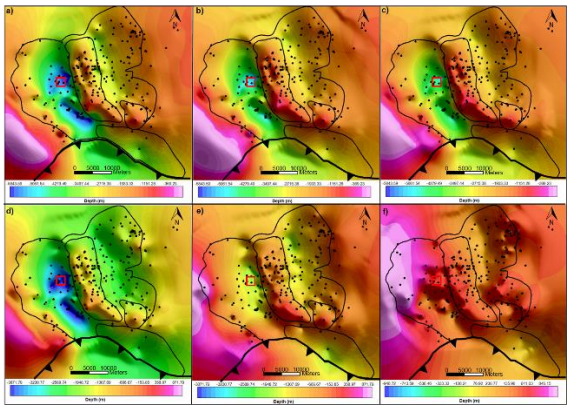

Fig 3: Summary of structural inputs used for gravity modeling. a) Top Ellenburger Formation, which reaches 6200 m below sea level beneath the central Delaware Basin. b) Top Devonian Formation. c) Top Barnett Formation. d) Top Strawn Formation. e) Top Lower Permian Formation that was partially eroded across the southern Central Basin Platform during early Permian. f) Top Rustler Formation. Black dots are the well control points. The study area is outlined by the small red box.

Results

The best density inversion of gravity (Tz) is achieved from the Combined layer (the fit between measured and modeled data converged after 126 inverse iterations), between topography and the top Leonardian formation, with a difference range of only -0.09 to 0.01mGal. The calculated gravity reveals more detail in the central part of study area: a subtle correlation with the Loving Fault in the southwestern study area, and a sharper bounding gradient of the anomaly high to the northeast over a possible unmapped regional fault system. The Combined layer inversion of Tzz also produced the best result (converged after 126 iterations). Differences between calculated and observed Tzz are less than 8 Eo (or 0.008 mGal/m). The statistical distribution of normalized differences between each observed and calculated gravity tensor after Tzz inversion show that Txz and Tyz tensor components are less variable compared to Tzz.

Following our examination of inversion results, we decided to use Tzz inversion of the combined layers to guide and map possible locations of hypogenic karst features. We improved this interpretation by focusing on calculated Txz and Tyz tensor components with their physical edge-defining character defined by the North-East-Down standard. Positive anomalies are highlighted with black lines related to northern edges of low-density source bodies and negative anomalies are highlighted with dashed black lines related to southern edges of low-density source bodies (Fig 4a, b). We then combined these directional results with the Tzz density inversion to interpret probable hypogenic karst locations (Fig 4d, e). The locations of low-density anomaly sources correlate well with the mapped source edges from Txz and Tyz components (Fig 4c, d, e). Density inversion results of the northeastern study region show fewer low-density anomaly sources; thus, they may be considered lower drilling risk locations (Fig 4). We conclude that the central and southwestern parts of the study area may encounter higher drilling risks, while the northeastern part of the study area is lower risk.

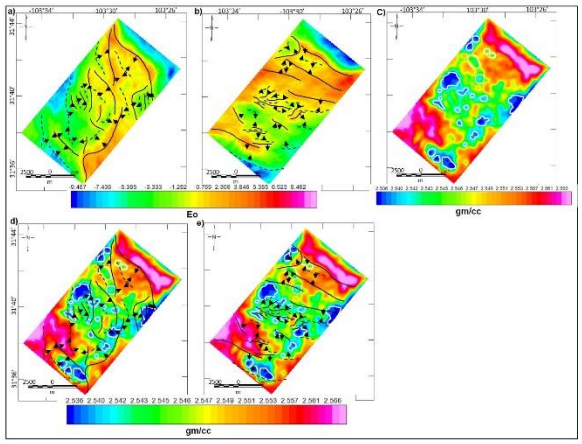

Fig 4: a) Calculated Txz anomalies from the Tzz density inversion on the Combined layer. Black lines trace positive anomalies and suggest an eastern low-density source body edge, while dashed black lines trace negative anomalies and suggest a western low-density source body edge. Arrows point towards low-density source bodies. b) Calculated Tyz from Tzz inversion on the Combined layer. Black lines trace positive anomalies and suggest a northern low-density source body edge, while dashed black lines trace negative anomalies and suggest a southern low-density source body edge. c) Inverted densities from Tzz density inversion on the Combined layer. Lower densities are outlined in white, correlating with the edges mapped in a) and b). d) Inverted densities with low-density outlines and mapped source edges from a). d) Inverted densities with low-density outlines and mapped source edges from b).

Conclusions

By integrating regional geological and geophysical controls with 3D FTG modeling, we are able to interpret regions lacking subsurface measurements due to karsting. We present a seldom used, but simple approach for interpreting the high-resolution gravity gradient data (FTG) and note that this integrated workflow may be applied to other regions that contain low-density geobodies. Low-density source body edges, outlined by measured Txz and Txy anomalies, indicate locations of possible hypogenic karst features. Integrating this approach with traditional 3D inverse density modeling of Tzz data clarifies the density distribution better than Tz density inversion alone, including steep gradients that suggest fault offsets.

Acknowledgments

We thank Bell Geospace for kindly providing the FTG data survey and Enverus for providing the well-log data used in this study. We thank Seequent for providing the educational license of the *Oasis montaj* software that was used for gravity modeling. We thank Scott Payton and Alan Morgan at Bell Geospace and Josh Sellars at Seequent for sharing their knowledge and insights. We thank the industry sponsors of the Conjugate Basins, Tectonics, and Hydrocarbons consortium at the University of Houston for their continuing support.

FTG application in karst features detection

Bell, R.E., Anderson, R., Pratson, L., 1997. Gravity gradiometry resurfaces. Lead. Edge 16 (1), 55–59.

Dutton, S. P., E. M. Kim, R. F. Broadhead, C. L. Breton, W. D. Raatz, S. C. Ruppel, and C. Kerans, 2004, Play analysis and digital portfolio of major oil reservoirs in the Permian Basin: Application and transfer of advanced geological and engineering technologies for incremental production opportunities, 1–428, https://www.osti .gov/servlets/purl/828411, accessed 15 January 2019.

Dutton, S. P., E. M. Kim, R. F. Broadhead, W. D. Raatz, C. L. Breton, S. C. Ruppel, and C. Kerans, 2005, Play analysis and leading-edge oil-reservoir development methods in the Permian Basin: Increased recovery through advanced technologies: AAPG Bulletin, 89, 553–576, doi: 10.1306/12070404093.

Ewing, T. E., 2019, Tectonics of the West Texas (Permian Basin) — Origins, structural geology, subsidence, and later modification, in S. C. Ruppel, ed., Anatomy of the Paleozoic basin: The Permian Basin, USA (vol.1, ch. 3): The University of Texas at Austin, Bureau of Economic Geology Report of Investigations 285: AAPG Memoir, 118, 63–96.

Majzoub, A.F., Stafford, K.W., Brown, W.A., Ehrhart, J.T., 2017. Characterization and delineation of gypsum karst geohazards using 2D electrical resistivity tomography in Culberson County, Texas, USA. J. Environ. Eng. Geophys. 22 (4), 411–420.

Morgan, R.A., Jorgensen, G., Payton, S., Stafford, K.W., 2018. Detection and Avoidance of Karst Related Shallow Geohazards Using Ultra High Resolution Full Tensor Gravity Gradiometry in the Delaware Basin, Texas. AAPG ACE Abstract.

Ruppel, S.C., Loucks, R., Kerans, C., Jones, R.H., Nance, H.S., Breton, C.L., Hamlin, S., Gale, J., Kane, J., McDonnell, A., Guevara, E., Wang, F., Reed, R., Wright, W., Rowe, H., Guven, N., Day-Stirrat, R., Jarvie, D., Zeng, H., Fu, Q., 2008. Permian Basin Synthesis Project: Data and Models for Recovering Existing and Undiscovered Oil Resources from the Largest Oil-Bearing Basin in the US GIS Dataset. http://www.beg.utexas.edu/research/areas/permian-basin-synthesis

Scholle, P.A., Goldstein, R.H., Ulmer-Scholle, D.S., 2004. Classic Upper Paleozoic Reefs and Bioherms of West Texas and New Mexico. New Mexico Institute of Mining and Technology, Socorro, NM, pp. 1–178.

Stafford, K. W., 2017, Hypogene evaporite karst of the greater Delaware Basin: *in*, Klimchouk, A., Palmer, A. N., De Waele, J., Auler, A. S., and Audra, P. (editors), *Hypogene karst regions and caves of the world*: Springer International Publishing, p. 531–542.

Stafford, K.W., Ehrhart, J.T., Majzoub, A.F., Shields, J.M. and Brown, W.A., 2018. Unconfined hypogene evaporite karst: West Texas and southeastern New Mexico, USA: International Journal of Speleology, v. 47, n. 3, p. 1-13.

Zhang, H., Mann, P., Bird, D. E., and Rudolph, K., 2021, Integration of regional gravity modeling, subsidence analysis, and source rock maturity data to understand the tectonic and hydrocarbon evolution of the Permian Basin, West Texas: Interpretation, v. 9, n. 1, p. T161-T181.